A Hierarchical Control Scheme for Residential Air-conditioning Loads to Provide Real-time Market Services under Uncertainties

Gayan Lankeshwara[a], Rahul Sharma [a,*], Ruifeng Yan[a], Tapan K. Saha[a]

[a]*School of Information Technology and Electrical Engineering, The University of Queensland, Brisbane, QLD 4072, Australia.*

Abstract

Recently, there has been growing interest in the provision of market services from distributed energy resources (DERs). In pursuing this goal, demand response (DR) aggregators continue to face challenges in retaining privacy and comfort for end-users, mitigating scalability issues while controlling a large cohort of DERs and handling uncertainties which are inevitable in a practical setting. This paper presents an end-user privacy and comfort preserving, scalable, hierarchical control scheme for inverter-type air conditioners to provide real-time market services in the presence of uncertainties. Privacy and scalability are achieved thorough the adoption of the alternating direction method of multipliers (ADMM) framework which ensures minimal reliance on local information whilst ensuring desired reference tracking without compromising the end-user comfort. Benefiting from the proposed non-conservative robust MPC design, the local control is able to account for mismatches in outdoor temperature predictions. The overall scheme is validated using real data obtained from the Australian Energy Market operator. The results demonstrate that the proposed approach can achieve desired tracking of the reference signal while regulating indoor temperature within a narrow range ($\pm 1^{\circ}$C) from the nominal set-point. Besides, the robustness to uncertainties is achieved without compromising computational performance and therefore the approach is scalable.

*Corresponding author

Email addresses: g.lankeshwara@uqconnect.edu.au (Gayan Lankeshwara), rahul.sharma@uq.edu.au (Rahul Sharma), ruifeng@itee.uq.edu.au (Ruifeng Yan), saha@itee.uq.edu.au (Tapan K. Saha)

Keywords: , Distributed energy resources (DERs), real-time market services, robust model predictive control (MPC), demand response (DR) aggregator, inverter-type air conditioners.

Notation

Throughout the paper, the following notation is practised. Bold-face letters represents multi-dimensional arrays. $\mathbb{R}$ represents the set of real numbers, $\mathbb{R}^n$ represents the space of n-dimensional vectors with real entries, $\mathbb{R}^{n\times m}$ represents the space of n by m matrices with real entries, $\mathbb{Z}_+$ represents the set of non-negative integers, $\mathbb{Z}_{[i,j]}$ represents the set of integers from i to j, $\mathbf{I}_n$ represents the $n\times n$ identity matrix, $\mathbf{1}_n$ represents a $n \times 1$ column vector consisting of ones, $\text{diag}\{x_1, \ldots, x_n\}$ is the diagonal matrix formed by $x_1, \ldots, x_n$ as its diagonal elements, $(\cdot)^{\mathrm{T}}$ represents the transpose operator, $|\cdot|$ is the absolute operator, $\|\cdot\|_2$ represents the ℓ_2-norm of a vector, $\wedge$ represents the logical AND operator, and $\mathbf{A}\otimes\mathbf{B}$ represents the Kronecker product of matrices $\mathbf{A}$ and $\mathbf{B}$.

1. Introduction

The global trend towards 'clean energy' has resulted in a dramatic increase in the penetration of renewables in the generation mix over the past decade [1]. Whilst solar and wind energy have gained dominance in this transformation, their highly intermittent nature has raised awareness among the network operators on the need for additional reserve capacity to sustain the grid during supply-demand imbalances.

Although preliminary reserve provisions were only limited to expensive conventional generation, the recent upgrades in bi-directional communication between end-users and the grid, sophisticated metering infrastructure have inspired the research community to explore the potential of 'behind-the-meter' distributed energy resources (DERs) in the provision of real-time market services [2].

The inherited high thermal inertia has made thermostatically controllable loads (TCLs) a promising DER candidate in the provision of electricity market services. To this end, a plethora of literature has been published by exploiting characteristic properties of TCLs in demand response (DR) and other market-based applications [3–18]. For instance, the authors in [3] have proposed a data-driven approach to optimise the total energy consumption of heating, ventilation, and air-conditioning (HVAC) where a multi-objective formulation accounts for the optimal tradeoff between energy consumption and thermal comfort. However, the approach is only

limited to demand management in a single facility. In [4], the authors have developed a feedback control mechanism and experimental validations have been conducted to evaluate the performance of variable-speed HVAC systems in delivering frequency regulation. Similar to [3], this study focuses only on achieving desired level performance with a single HVAC unit. Conversely, the authors in [5] have utilised a ranking mechanism for an aggregate population of household air conditioners based on their operating temperature for dispatch during a frequency regulation event. Following a similar approach, the authors in [6] have presented a stochastic-battery model and thereby employ a priority-stacked control scheme for TCLs to track a regulation signal. Furthermore, the authors in [7] have implemented a model predictive control (MPC) scheme for aggregate control of variable-speed air conditioners where the performance metrics are aligned with tracking the reference set-point signal and minimising thermal discomfort for end-users. However, the authors assume perfect knowledge of individual thermal characteristics of TCLs and accurate ambient temperature forecasts.

On the contrary, the authors in [8] have presented a centralised approach for the control of TCLs where the uncertainty in ambient temperature is addressed via a stochastic scenario-based optimisation approach. In addition to that, a stochastic chance constrained MPC approach is proposed in [9] for building climate control while addressing the variation in outdoor temperature. Furthermore, the authors have utilised an affine disturbance feedback control policy to obtain a tractable solution to the stochastic MPC problem. However, stochastic optimisation approaches often require the distribution of uncertainty to be known as a priori, for example, outdoor temperature variation is assumed to follow a gaussian distribution in [9]. Nonetheless, the distribution of uncertainty is hardly known for most of the real-world applications [19] and therefore restricting the uncertainty to follow a certain distribution often undermines the performance in a real-world setting. On the other hand, stochastic optimisation approaches also require a significant number of scenarios to model the uncertainty set [19], which is often computationally prohibitive in the context of aggregate control of DERs.

To this end, the majority of the control approaches rely on a centralised control framework, e.g., direct load control, where a DR aggregator has the sole authority to control the entire population of consumer-owned DERs. Nonetheless, such centralised schemes suffer from serious limitations due to: end-user privacy violations; inevitable scalability issues under large-scale aggregations of consumer-owned devices [20]. Hence, it is undoubted that a control approach which meets the expectations of the DR aggregator as well as the end-user is vital for an enticing implementation in the provision of real-time market services.

An alternative to centralised control is to implement distributed control [20] whereby each DER is managed by a local controller. To date, several studies have proposed distributed control schemes for TCLs to provide DR and electricity market services [10–18]. For example, the authors in [10] have proposed a hierarchical optimal control strategy for HVAC systems to provide regulation services. Furthermore, the approach considers the tradeoff between economic interests and thermal comfort without violating operational constraints of HVAC systems. Nonetheless, perfect thermodynamic models of HVAC systems are considered in developing the overall control framework. In [11], the authors have proposed a fully-decentralised coordinated control approach to control heats pumps with the objective of minimising household surplus energy. Although end-user privacy is preserved, reliance on neighbour-neighbour communication makes the approach impracticable in a real-world setting. The authors in [12] have presented a privacy-preserving iterative control approach where households communicate with a central controller. Despite the applicability in energy arbitrage and congestion management, the proposed method has failed to address the inaccuracies in household demand profiles shared with the central controller.

In [13], a receding-horizon distributed control approach is presented to deliver ancillary services from TCLs. In this approach, each distributed agent is responsible for monitoring and control of a small group of devices, hence there is no guarantee that privacy is fully preserved at device level. In [14], a method to regulate supply-demand balance with a price mechanism is developed with distributed MPC and dual decomposition. Nevertheless, the poor convergence characteristics of the dual decomposition method [21] undermines the overall performance of the distributed control scheme in providing real-time services. A decentralised control scheme for ON-OFF type air conditioners based on stochastic control is introduced in [15]; however, the aperiodic nature of the desired power curves for individual air conditioners makes the approach inapplicable for real-time market services. Apart from that, the control approach is also inconsistent with variable-speed air conditioners where the power consumption is not limited to either ON or OFF. The authors in [16] have proposed an Alternating Direction Method of Multipliers (ADMM) based hierarchical control scheme for TCLs to follow a generation signal; however, the uncertainties present in a practical setting are not explicitly considered in the implementation of the control scheme. Furthermore, the offline-optimisation based approach is only suited for providing services in day-ahead markets. In [17], the authors have presented a distributed control approach for TCLs based on Douglas-Rachford splitting. Despite the generalisation of the overall control approach under diverse performance metrics, the

authors have failed to carry out a thorough analysis for a particular scenario while accounting for uncertainties in real-world implementation.

In a different study [18], the authors have presented a hierarchical control scheme based on MPC and ADMM for day-ahead and intra-day control of electro-thermal devices. In this study, the uncertainty in thermal demand is modelled via a robust optimisation approach where the bounds (range forecasts) of thermal demand are assumed to be known. Thereafter, the concept of *'uncertainty budgets'* [22] is utilised to appropriately tune the robustness of the approach to avoid unnecessary conservatism associated with the conventional robust optimisation technique [23]. Nevertheless, the overall approach is a single-stage process (without *recourse*) and all the control decisions are required to be made before the uncertainties are revealed at a certain time instant. In this regard, setting the robustness parameter at the most appropriate level is vital to obtain desired outcomes of the overall control implementation. This is challenging as there is always a trade-off between the desired performance and resiliency to uncertainties. On the other hand, the application of ADMM to achieve generation-consumption balance among electro-thermal devices in this context is different from our approach where air conditioners sufficiently adjust their consumption to follow a load set-point signal. A summary of the literature on distributed control of DERs is given in Table 1.

Table 1. A comparison of the existing literature on distributed control of behind-the-meter DERs

Ref.	**control approach**	**privacy**	**uncertainties addressed?**
Wang et al. [10]	regulation bidding controller+ power use following controller	◐	×
Dengiz et al. [11]	Iterative Desync Algorithm	●	×
Dong et al. [12]	an iterative algorithm	●	×
Radaideh et al. [13]	tracking problem + receding-horizon control	●	×
Larsen et al. [14]	MPC + dual decomposition	◐	×
Tindemans et al. [15]	decentralised stochastic control	●	×
Burger et al. [16]	ADMM + offline optimisation	●	×
Halvgaard et al. [17]	MPC + Douglas Rachford splitting	●	×
proposed	*ADMM + robust MPC*	●	✓

● = fully considered; ◐ = partially considered; × = not considered;

The existing literature suggests that distributed DER control schemes have the potential to mitigate end-user data privacy concerns and scalability issues while achieving the same level of performance of centralised control schemes. However, ignoring the effects of uncertainties in such a distributed control setting is detrimental for DR aggregators when providing services in real-time electricity markets. On the one hand, addressing uncertainties in distributed control schemes via traditional robust optimisation techniques [23] result in extremely conservative control approaches which a DR aggregator participating in real-time markets usually avoids. On the other hand, addressing conservatism in such approaches might lead to intractable problems; hence, unscalable in a practical setting. To this end, a tractable approach for distributed control of DERs under uncertainties is highly favoured by retailers and DR aggregators to provide real-time market services. Not only that, the majority of the control schemes based on air-conditioning loads predominantly focus on achieving desired control from regular ON-OFF type air conditioners even though there is a growing demand for inverter-type air conditioners [24].

Fig. 1 illustrates key aspects of the proposed hierarchical control scheme as opposed to a centralised control approach for the provision of real-time market services from TCLs under uncertainties.

Motivated by the knowledge gap and to enhance the real-world implementation capability of TCLs to provide real-time market services, the major contributions of this work can be stated as follows:

- Developing an end-user privacy and thermal comfort preserving, hierarchical control scheme for DR aggregators to provide real-time services in electricity markets. The approach is developed using ADMM such that local controllers in individual households optimise their economic interests whilst a coordinating controller at the DR aggregator ensures precise tracking of the load set-point signal.

- Addressing uncertainties associated with imperfect outdoor temperature forecasts at each household local controller level via a non-conservative and computationally tractable robust control approach. To this end, a closed-loop MPC scheme coupled with a causal disturbance feedback control policy is utilised.

- Ensuring the overall control scheme to be consistent with the operation of modern inverter-type air conditioners.

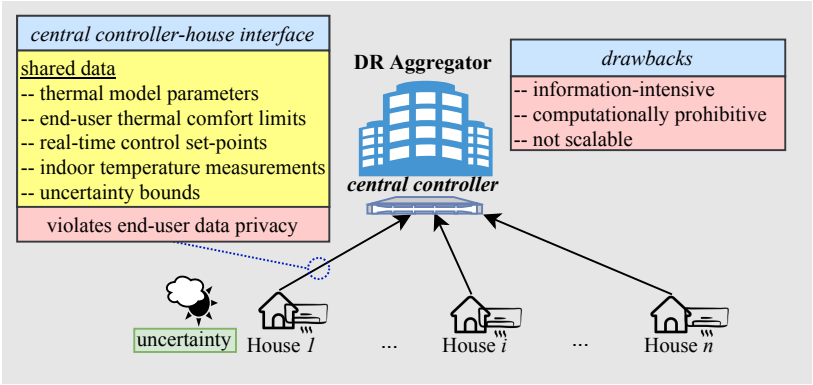

(a) Centralised control approach

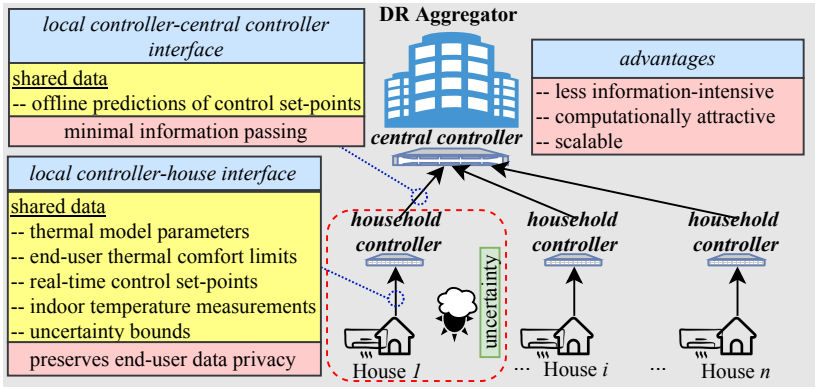

(b) Proposed hierarchical control approach

Fig. 1. A comparison of the (a) centralised control approach and (b) proposed hierarchical control approach for the control of TCLs under uncertainties (for simplicity, illustrations are only provided for House 1).

The rest of the paper is organised as follows. Section 2 introduces the system model and formulates the overall control problem. Section 3 describes the proposed hierarchical robust control framework based on ADMM and robust MPC. Section 4 outlines simulation results and section 6 concludes the paper.

2. System Model and Problem Description

2.1. Individual model

In this work, the provision of real-time market services is achieved from inverter-type air conditioners. Compared to regular ON-OFF type air conditioners, inverter-type air conditioners are capable of operating under continuous power levels [25].

Assuming slow thermal dynamics relative to power tracking dynamics, a linearised thermal model adopted from [26] and validated with experimental results as in [27, 28] is utilised to develop the state-space model of an air-conditioning system. For the *i*th inverter-type air conditioner, this can be expressed as:

$$x_i(k+1) = A_i\, x_i(k) + B_i\, u_i(k) + D_i\, \tilde{v}_i(k) + w_i(k) \tag{1a}$$

$$y_i(k) = x_i(k) \tag{1b}$$

where k is the sampling instant, the state $x_i(k) \in \mathbb{R}$ represents indoor temperature $T_i(k)$; control input $u_i(k) \in \mathbb{R}$ represents power consumption $P_i(k) \in [\,\underline{P}_i,\, \overline{P}_i\,]$, where $\underline{P}_i$ is the minimum power consumption; $\overline{P}_i$ is the rated consumption; external input $\tilde{v}_i(k) \in \mathbb{R}$ corresponds to the nominal outdoor temperature $\tilde{T}_i^{\text{out}}(k)$ and $w_i(k) \in \mathbb{R}$ is the stochastic additive disturbance term associated with the uncertainty in outdoor temperature. Considering full-state feedback, output $y_i(k) \in \mathbb{R}$ corresponds to measured indoor temperature. In addition to that, $A_i, B_i, D_i \in \mathbb{R}$ such that $A_i = e^{-\Delta/R_iC_i}$, $B_i = R_i \cdot \left(1 - e^{-\Delta/R_iC_i}\right)$ and $D_i = \left(1 - e^{-\Delta/R_iC_i}\right)$, where R_i is the thermal resistance, C_i is the thermal capacitance and Δ is the sampling period.

Considering actual outdoor temperature v_i to be a symmetric range forecast centred at $\tilde{v}_i$ such that: $v_i \in [\tilde{v}_i - \hat{v}_i,\ \tilde{v}_i + \hat{v}_i]$, where $\hat{v} > 0$ is the semi-amplitude of the maximum variation related to the uncertainty associated with v_i, the bounded uncertainty set for w_i can be obtained as:

$$\mathbb{W}_i = \{w_i :\ |w_i| \leq D_i \cdot \hat{v}_i\} \tag{2}$$

2.2. Aggregate model

Let n be the size of the population of inverter-type air conditioners indexed by i. Since the dynamics of each air conditioning subsystem is independent of others, the dynamics of the aggregate system can be represented as a stacked system of individual models. This can be expressed as:

$$\mathbf{x}(k+1) = A\,\mathbf{x}(k) + B\,\mathbf{u}(k) + D\,\tilde{\mathbf{v}}(k) + G\,\mathbf{w}(k) \tag{3a}$$

$$\mathbf{y}(k) = E\,\mathbf{x}(k) \tag{3b}$$

where $\mathbf{x}(k) = \left[x_1(k) \cdots , x_n(k)\right]^{\mathrm{T}}$, $\mathbf{u}(k) = \left[u_1(k) \cdots , u_n(k)\right]^{\mathrm{T}}$, $\tilde{\mathbf{v}}(k) = \left[\tilde{v}_1(k) \cdots , \tilde{v}_n(k)\right]^{\mathrm{T}}$, $\mathbf{y}(k) = \left[y_1(k) \cdots , y_n(k)\right]^{\mathrm{T}}$ and $\mathbf{w}(k) = \left[w_1(k) \cdots , w_n(k)\right]^{\mathrm{T}}$. In addition to that, $A = diag\{A_i\}$, $B = diag\{B_i\}$, $D = diag\{D_i\}$ for $i = \{1, \ldots, n\}$, $G = \mathbb{I}_n$ and $E = \mathbb{I}_n$.

2.3. Problem Description

The goal of this work is to develop a robust control scheme for the provision of real-time market services from residential air conditioners in the presence of uncertainties. Aligned with this, it is assumed that the bids offered by the DR aggregator in day-ahead markets are accepted prior to the event.

Let us consider a scenario where the DR aggregator receives a load set-point reference signal P_{ref} that should be tracked for T_{dur} of time. Following this, the DR aggregator utilises robust min-max MPC for the provision of real-time market services in the presence of uncertainties.

Considering the prediction horizon to be $N \in \mathbb{Z}_+$, the state prediction vector for the aggregate system can be expressed as:

$$\mathbf{x}(k) = \left[\mathbf{x}^{\mathrm{T}}(k|k) \ldots, \mathbf{x}^{\mathrm{T}}(k+N|k)\right]^{\mathrm{T}} \in \mathbb{R}^{n(N+1)} \tag{4}$$

where the notation $\mathbf{x}(\cdot)(k+j|k)$ refers to the prediction of $\mathbf{x}$ in $(k+j)$th sampling instant with the knowledge of information up to kth sampling instant. Following a similar approach, the other vectors in the state space model can be expressed as given in Appendix A.

Thereafter, the state prediction dynamics of the aggregate system can be expressed in a compact form as:

$$\mathbf{x}(k) = \mathbf{A}\,\mathbf{x}(k|k) + \mathbf{B}\,\mathbf{u}(k) + \mathbf{D}\,\tilde{\mathbf{v}}(k) + \mathbf{G}\,\mathbf{w}(k) \tag{5a}$$

$$\mathbf{y}(k) = \mathbf{E}\,\mathbf{x}(k) \tag{5b}$$

where $\mathbf{A} \in \mathbb{R}^{n(N+1)\times n}, \mathbf{B}, \mathbf{D}, \mathbf{G} \in \mathbb{R}^{nN\times nN}$ and $\mathbf{E} \in \mathbb{R}^{n(N+1)\times nN}$ matrices are given in Appendix B.

On the other hand, the design objective of the MPC controller at the DR aggregator is considered to be minimising the linear cost of power consumption of associated with air conditioners expressed as the stage cost:

$$\ell_j\Big(\mathbf{x}(k+j|k), \mathbf{u}(k+j|k)\Big) = \mathbf{\Lambda}^{\mathrm{T}}(k+j|k) \cdot \mathbf{u}(k+j|k), \quad \forall\, j \in \mathbb{Z}_{[0,N-1]} \tag{6}$$

where $\mathbf{\Lambda}(k+j) \in \mathbb{R}^n$ is the electricity price vector for the houses at $(k+j)$th sampling instant. The price vector can be either time-of-use tariffs or real-time prices [29]. Taken together, the robust min-max MPC control problem at the DR aggregator can be expressed as:

$$\min_{\mathbf{u}} \quad \max_{\mathbf{w}} \quad \sum_{j=0}^{N-1} \ell_j\Big(\mathbf{x}(k+j|k), \mathbf{u}(k+j|k)\Big) \tag{7a}$$

subject to:

$$\mathbf{x}(k) = \mathbf{A}\,\mathbf{x}(k|k) + \mathbf{B}\,\mathbf{u}(k) + \mathbf{D}\,\tilde{\mathbf{v}}(k) + \mathbf{G}\,\mathbf{w}(k) \tag{7b}$$

$$\mathbf{y}(k) = \mathbf{E}\,\mathbf{x}(k) \tag{7c}$$

$$\underline{\mathbf{y}} \leq \mathbf{y}(k+j|k) \leq \overline{\mathbf{y}}, \qquad \forall\, j \in \mathbb{Z}_{[0,N-1]} \tag{7d}$$

$$\underline{\mathbf{u}} \leq \mathbf{u}(k+j|k) \leq \overline{\mathbf{u}}, \qquad \forall\, j \in \mathbb{Z}_{[0,N-1]} \tag{7e}$$

$$\mathbf{1}_n^{\mathrm{T}} \cdot \mathbf{u}(k+j|k) = P_{\mathrm{ref}}(k+j|k), \qquad \forall\, j \in \mathbb{Z}_{[0,N-1]} \tag{7f}$$

$$\mathbf{w}(k+j|k) \in \mathcal{W}, \qquad \forall\, j \in \mathbb{Z}_{[0,N-1]} \tag{7g}$$

In the open-loop min-max MPC implementation, (7a) corresponds to minimising the cost of consumption of electricity under the worst-case uncertainty associated with outdoor temperature. The state-space model of the aggregate system is described by (7b) and (7c). The indoor thermal comfort limits are described by (7d), where $\underline{\mathbf{y}} = [\underline{y}_1, \ldots, \underline{y}_n]^{\mathrm{T}} \in \mathbb{R}^n$ refers to the preferred lower set-point and $\overline{\mathbf{y}} = [\overline{y}_1, \ldots, \overline{y}_n]^{\mathrm{T}} \in \mathbb{R}^n$ corresponds to the preferred upper set-point of indoor temperature. The constraints on the power consumption of air conditioners are given by (7e), where $\underline{\mathbf{u}} = [\underline{u}_1, \ldots, \underline{u}_n]^{\mathrm{T}} \in \mathbb{R}^n$ is the lower limit of power consumption and $\overline{\mathbf{u}} = [\overline{u}_1, \ldots, \overline{u}_n]^{\mathrm{T}} \in \mathbb{R}^n$ is the upper-limit of power consumption (rated consumption) for the population of air conditioners. Tracking of the reference set-point signal P_{ref} at each sampling instant is given by the hard constraint (7f). In addition to that, (7g) describes the bounded, priori known set $\mathcal{W} \subset \mathbb{R}^n$, for which the uncertainty associated with the prediction of outdoor temperature of each house belongs to.

Nonetheless, the implementation of the robust receding horizon control implementation (7) at the DR aggregator is challenging due to:

- privacy violations as end-users are required to share information pertaining to rated capacity of air conditioners, preferred indoor thermal comfort limits $(\underline{y}_i, \overline{y}_i\, \forall\, i)$ and household thermal characteristics, i.e, $(R_i, C_i)\, \forall\, i$, with the DR aggregator.

- full-state feedback associated with (7c) requires end-users to share real-time or near real-time measurements of indoor temperature with the DR aggregator for the entire control period. This also leads to end-user privacy violations.

- with the aggregation of a large number of end users (large n) to be able to participate in real-time market services, the robust min-max MPC formulation (7) generally leads to an intractable problem [30].

Hence, an end-user privacy guaranteed, scalable and computationally tractable control approach is proposed for the real-time provision of market services from residential air conditioning loads under uncertainties.

3. Proposed Methodology

The overall idea is to develop a hierarchical control scheme which alleviates privacy and scalability issues and at the same time mitigates the effects of external sources of uncertainty. A summarised block diagram of the overall control approach is given in Fig. 2.

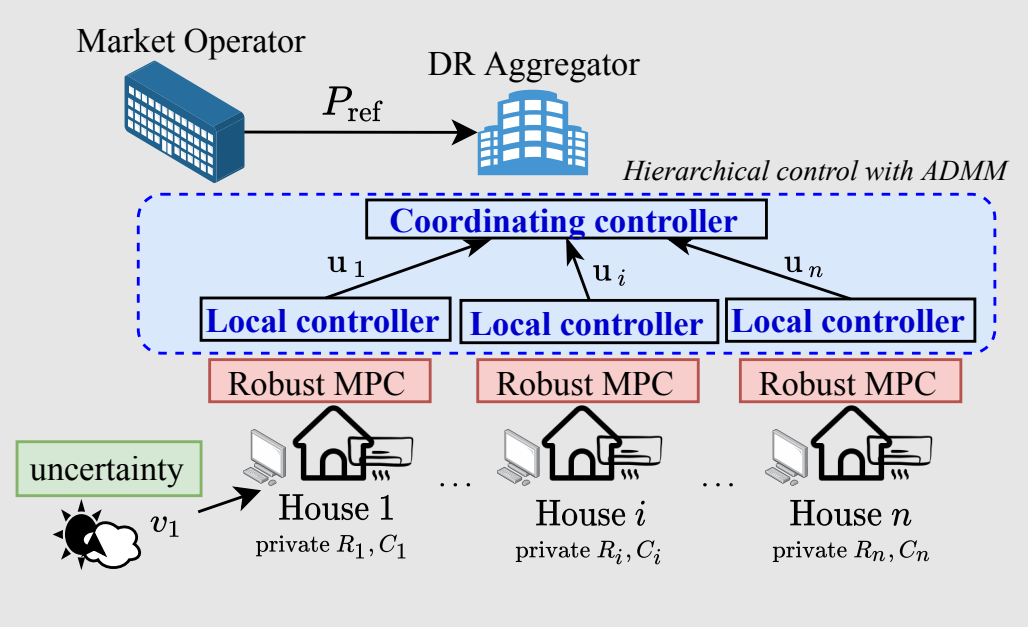

Fig. 2. A summarised block diagram of the overall control framework: local controllers at each household and the coordinating controller at the DR aggregator are derived from decomposition based on ADMM; derived local controllers employ robust MPC to account for uncertainties in outdoor temperature v (only shown for House 1).

Based on a high-level view, the approach taken in this paper can be described under three sections: transforming the centralised problem to its decentralised form with ADMM; developing a computationally tractable, robust MPC scheme coupled with a causal disturbance feedback policy at each local controller to address uncertainties associated with outdoor temperature; establishing the coordi-

nation between local controllers and the DR aggregator via a coordinating controller to achieve precise tracking of the reference set-point signal.

3.1. Decentralised alternative formulation based on ADMM

The control problem in section 2.3 is analogous to a typical *resource sharing* problem due to the power balance constraint (7f). In the absence of (7f), the solution to original problem (7) can be obtained by solving a set of subproblems at individual households. Hence, ADMM technique [31] is utilised to transform the centralised control problem to its equivalent decentralised form. The main reason behind the selection of ADMM is its superior convergence characteristics compared to other classical decomposition techniques [20].

In standard form, the *resource sharing* problem can be expressed as,

$$\min_{\mathbf{u}_1,\ldots,\mathbf{u}_n} \quad \sum_{i=1}^{n} \ell_i(\mathbf{u}_i) + g\Big(\sum_{i=1}^{n} \mathbf{u}_i\Big) \tag{8}$$

where n is the number of individual subsystems, the decision variables are $\mathbf{u}_i \in \mathbb{R}^m$ for $i = 1, \ldots, n$, $\ell_i : \mathbb{R}^m \to \mathbb{R}$ is the local cost function for the ith subsystem and $g : \mathbb{R}^{m\times n} \to \mathbb{R}$ is the shared objective term which takes $\sum_i^n \mathbf{u}_i$ as an argument. In other words, (8) represents a problem in which the local agent i minimises its individual cost $\ell_i(\mathbf{u}_i)$, while minimising the shared objective $g(\sum_{i=1}^{n} \mathbf{u}_i)$ among all local agents.

The scaled form of the ADMM for the *sharing problem* for νth iteration can be expressed as follows [31]:

$$\mathbf{u}_i^{(\nu+1)} = \underset{\mathbf{u}_i}{\operatorname{argmin}} \Big(\ell_i(\mathbf{u}_i) + (\rho/2) \Big\| \mathbf{u}_i - \mathbf{u}_i^{(\nu)} + \overline{\mathbf{u}}^{(\nu)} - \overline{\mathbf{z}}^{(\nu)} + \boldsymbol{\theta}^{(\nu)} \Big\|_2^2 \Big) \tag{9}$$

$$\overline{\mathbf{z}}^{(\nu+1)} = \underset{\overline{\mathbf{z}}}{\operatorname{argmin}} \Big(g(n\,\overline{\mathbf{z}}\Big) + (n\rho/2) \Big\| \overline{\mathbf{z}} - \boldsymbol{\theta}^{(\nu)} - \overline{\mathbf{u}}^{(\nu+1)} \Big\|_2^2 \Big) \tag{10}$$

$$\boldsymbol{\theta}^{(\nu+1)} = \boldsymbol{\theta}^{(\nu)} + \overline{\mathbf{u}}^{(\nu+1)} - \overline{\mathbf{z}}^{(\nu+1)} \tag{11}$$

where superscript (ν) represents νth iteration, $\rho > 0$ is the augmented Lagrangian parameter, $\overline{\mathbf{u}}$ is the average of $\mathbf{u}_i$, $\overline{\mathbf{z}} \in \mathbb{R}^m$ is an auxillary variable such that $\overline{\mathbf{z}} = (1/n)\sum_{i=1}^{n} \mathbf{z}_i$ and $\boldsymbol{\theta} \in \mathbb{R}^m$ is the global scaled-dual variable.

In the context of the problem addressed in this work, the control action at each local controller present in each household can be identified by (9). This can be executed individually in parallel based on a local design objective l_i for all i. On the other hand, (10) and (11) can be implemented on a coordinating controller

(the mediating agent) whose primary goal is to achieve perfect tracking of the load set-point signal at each sampling instant. This is governed by the shared objective:

$$g\Big(\sum_{i=1}^{n} u_i(k)\Big) = \Big(\sum_{i=1}^{n} u_i(k) - P_{\text{ref}}(k)\Big)^2, \quad \forall\, k \tag{12}$$

In this manner, the control problem for the DR aggregator in section 2.3 can be transformed into a hierarchical control problem with a local controller at each household and a coordinating controller at the DR aggregator. It is worth mentioning here that, since g is chosen to be convex as in (12), choosing $f_i,\ \forall i$ to be convex results in proper convergence of the ADMM scheme [31].

3.2. Local controller

Following the hierarchical control framework based on ADMM, the conventional approach would be to implement robust min-max MPC at each controller to assign control set-points for the air conditioner while taking account of fluctuations in outdoor temperature. However, such an open loop control approach is overly conservative and unrealistic [30] as the local controller determines air conditioner set-points for the whole prediction horizon considering worst-case uncertainty associated with outdoor temperature at every future time step.

To address this issue, a closed loop MPC approach with a causal disturbance feedback policy of the form $\mu_{k+j|k}(w(k|k), \ldots, w(k+j-1|k))$ is utilised [32]. Considering the ith air conditioning subsystem, the causal disturbance feedback control policy can be mathematically expressed as:

$$u_i(k+j|k) = \sum_{m=0}^{j-1} \mathrm{T}_i(k+j|k, k+m|k) \cdot w_i(k+m|k) + \tilde{u}_i(k+j|k) \quad \forall\, j \in \mathbb{Z}_{[0,N-1]} \tag{13}$$

where $\mathrm{T}_i(k+j\,|\,k, k+m\,|\,k) \in \mathbb{R}$ and $\tilde{u}_i(k+j\,|\,k) \in \mathbb{R}$ are the decision variables associated with the policy. This approach is similar to the concept of '*recourse*' in multi-stage problems commonly discussed under *affinely adjustable robust optimisation* [33]. Based on (13), the control decision at the current step $u_i(k)$ is only determined with optimisation ("here-and-now" decisions) and future control decisions $u_i(k+j)\ \forall\ j \in \mathbb{Z}_{[0,N-1]}$ (which are affine functions of w_i) are revealed only after the uncertainties $w_i(k+m)\ \forall\, m \in \mathbb{Z}_{[0,j-1]}$ are realised with the availability of full-state feedback ("wait-and-see" decisions). In other words, the decision on the current input is independent of uncertainties whereas all future inputs are dependent on yet unknown disturbances. Unlike the traditional approach where future input decisions are determined based on worst possible uncertainties at each

step, this approach alleviates the conservatism whereby future input decisions are determined only after the disturbances are determined.

Since the first input which is unaffected by uncertainties is only optimised, the stage cost of the local controller problem is slight modified to consider the uncertainty-free inputs as:

$$\ell_{i,j}\Big(x_i(k+j\,|\,k), \tilde{u}_i(k+j\,|\,k)\Big) = \Lambda_i\,(k+j\,|\,k)\cdot \tilde{u}_i(k+j\,|\,k), \quad \forall\, i\,, \forall\, j \in \mathbb{Z}_{[0,N-1]} \tag{14}$$

where $\tilde{u}_i(k+j\,|\,k) \in \mathbb{R}$ is the uncertainty-free input at $(k+j)$th sampling instant obtained from (13); $\Lambda_i\,(k+j\,|\,k) \in \mathbb{R}$ is the electricity price at $(k+j)$th sampling instant for the ith air conditioner.

Hence, the closed-loop MPC problem for the ith local controller, LC_i, after applying ADMM for νth iteration at kth sampling instant can be expressed as:

$$\begin{aligned}\min_{\mathbf{T}_i,\,\tilde{\mathbf{u}}_i} \quad \max_{\mathbf{w}_i} \quad & \sum_{j=0}^{N-1}\Big[\,\ell_{i,j}\Big(x_i(k+j\,|\,k), \tilde{u}_i(k+j\,|\,k)\Big) \\ & + (\rho/2)\Big(\tilde{u}_i(k+j|k) - \tilde{u}_i^{(\nu)}(k+j) + \overline{\tilde{u}}^{\,(\nu)}(k+j) - \overline{z}^{(\nu)}(k+j) + \theta^{(\nu)}(k+j)\Big)^2\Big]\end{aligned} \tag{15a}$$

subject to:

$$\mathbf{x}_i(k) = \mathbf{A}_i\,\mathbf{x}_i(k\,|\,k) + \mathbf{B}_i\,\mathbf{u}_i(k) + \mathbf{D}_i\,\tilde{\mathbf{v}}_i(k) + \mathbf{w}_i(k) \tag{15b}$$

$$\mathbf{y}_i(k) = \mathbf{E}_i\,\mathbf{x}_i(k) \tag{15c}$$

$$\underline{y_i} \le y_i(k+j\,|\,k) \le \overline{y_i}, \qquad \forall\, j \in \mathbb{Z}_{[0,N-1]} \tag{15d}$$

$$\underline{u_i} \le u_i(k+j\,|\,k) \le \overline{u_i}, \qquad \forall\, j \in \mathbb{Z}_{[0,N-1]} \tag{15e}$$

$$w_i(k+j\,|\,k) \in \mathbb{W}_i, \qquad \forall\, j \in \mathbb{Z}_{[0,N-1]} \tag{15f}$$

$$u_i(k+j\,|\,k) = \mu_{i,k+j\,|\,k}\,(w(k\,|\,k), \ldots, w(k+j-1\,|\,k)), \qquad \forall\, j \in \mathbb{Z}_{[0,N-1]} \tag{15g}$$

The cost function in (15a) is derived from the ADMM decomposition given in (9). Aligned with the causal disturbance feedback policy (13), the ADMM decision variable is also chosen to be $\tilde{u}_i$ rather than the original decision variable u_i. The state prediction dynamics for the ith subsystem are given by (15b) and (15c). The output and input constraints are given by (15d) and (15e) respectively. The set to which the uncertainty in outdoor temperature of ith air conditioning subsystem belongs to is described by (15f) and the bounded set $\mathbb{W}_i$ is obtained from (2). The

causal disturbance feedback control policy for the ith subsystem is represented by (15g).

Aligned with the nature of uncertainty associated with outdoor temperature given by (2), the closed-loop MPC problem described by (15) can be formulated as a convex quadratic programming problem (the derivation is given in Appendix C). Subsequently, the problem at the local controller is computationally tractable and can be easily solved with off-the-shelf solvers as compared to the centralised control approach (7).

3.3. Coordinating controller

While each local controller minimises the cost of consumption of electricity associated with the air conditioner, the objective of the coordinating controller is to achieve desired tracking of the load set-point signal. In the context of ADMM algorithm employed in this study, this can be realised with: 1) performing the z-update similar to (10); 2) performing the θ-update similar to (11). Additionally, aligned with the receding horizon implementation, the control problem for the coordinating controller for νth iteration at kth sampling instant can be mathematically expressed as:

$$\min_{\bar{\mathbf{z}}} \sum_{j=0}^{N-1} \left[g(n\bar{z}(k+j)) + (n\rho/2) \left\| \bar{z}(k+j) - \theta^{(\nu)}(k+j) - \bar{\tilde{u}}^{(\nu+1)}(k+j) \right\|_2^2 \right] \tag{16a}$$

$$\theta^{(\nu+1)}(k+j) = \theta^{(\nu)}(k+j) + \bar{\tilde{u}}^{(\nu+1)}(k+j) - \bar{z}^{(\nu+1)}(k+j), \quad \forall\, j \in \mathbb{Z}_{[0,N-1]} \tag{16b}$$

3.4. Convergence of the algorithm

Aligned with [31], the termination criteria for the receding horizon implementation of the *sharing problem* in ADMM form at kth sampling instant can be expressed as:

$$\| \mathbf{r}^{(\nu)}(k) \|_2 \leq \epsilon^r, \quad \| \mathbf{s}^{(\nu)}(k) \|_2 \leq \epsilon^s, \quad \forall\, k \tag{17}$$

where $\mathbf{r}$ and $\mathbf{s}$ are the primal residual and dual residual as defined in Appendix D, $\epsilon^r > 0$ and $\epsilon^s > 0$ are the tolerances for the primal residual and dual residual respectively.

Fig. 3 depicts the sequential information and control flow between local controller LC_i and the coordinating controller for at a certain sampling instant, let's say k. According to ① in Fig. 3, LC_i determines the uncertainty-immunised predicted control sequence $\tilde{u}_i^{(\nu)}(k+j)$ for $j \in \mathbb{Z}_{[0,N-1]}$, for νth iteration after solving the closed loop MPC problem (15) and thereafter sends to the coordinating

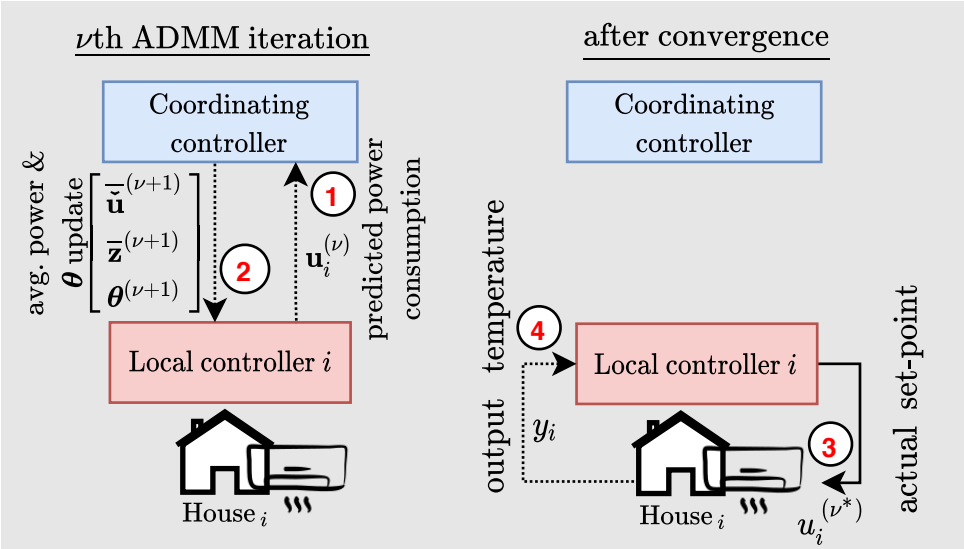

Fig. 3. The hierarchical control scheme depicting the control and information flow between ith local controller (LC_i) and the coordinating controller; only LC_i is shown for clarity; solid lines represent control flow; dotted-lines represent information flow; numbered-circles represent the sequence of steps

controller. With similar information from all i, the coordinating controller calculates the average $\overline{\tilde{u}}^{(\nu+1)}(k+j)$ for $j \in \mathbb{Z}_{[0,N-1]}$ and determines $\overline{z}^{(\nu+1)}(k+j)$ by solving (16a). In the next step, $\theta^{(\nu+1)}(k+j)$ is calculated as in (16b). Thereafter, $\left[\overline{u}^{(\nu+1)}(k+j), \overline{z}^{(\nu+1)}(k+j), \theta^{(\nu+1)}(k+j)\right]$ is scattered among all the local controllers as in ②. This back-and-forth information sharing between a local controller and a coordinating controller occurs until the termination criteria (17) is met. Let us say that convergence is met at ν^*th iteration of the ADMM scheme. Subsequently, the local controller applies the first control input of the predicted sequence $\tilde{u}_i^{(\nu^*)}(k+j)$ to the ith air-conditioning subsystem as in ③. With full-state feedback, in the next step, LC_i measures the indoor temperature $y_i(k)$ and updates the system as shown in ④. Likewise, this procedure is repeated at each sampling instant until the end of the demand management event.

It should be noted that this work assumes the existence of two-way communication between household local controllers and the coordinating controller via a direct wired link such as copper, optical fibre or a wireless link such as microwave [34]. These communication links can be utilised to send control signals and receive information from local controllers. Furthermore, the communication link is

assumed to be perfect, i.e., free from bandwidth limitations and latency issues.

Some remarks about the key features of the proposed approach are as follows:

Remark (Privacy of end-users)**.** *Since each local controller acts as an intermediary between the house and the DR aggregator, a household does not need to share sensitive information ($R_i, C_i \; \forall \; i$) with the DR aggregator as in the control approach* (7)*. Instead, information is only shared with the local controller built in its own premises. On the other hand, the deployment of local controllers eliminate the requirement of state-estimation techniques [26, 35] for the DR aggregator to measure indoor temperature for all the air conditioners. On the contrary, our approach is more realistic in the sense that only local controllers have full-state feedback capabilities to measure indoor temperature. Apart from that, our approach relies on a coordinating controller to share minimal information, for example, offline predictions of air conditioner control set-points $\tilde{u}_i^{(\nu)}(k+j)$ for $j \in \mathbb{Z}_{[0,N-1]} \; \forall \; i$, and therefore does not require interactions among neighbouring local controllers. This is in contrast to [17, 36] where the overall control implementation heavily depends on interactions among local controllers. By means of aforementioned strategies, it is guaranteed that end-user data privacy is preserved.*

Remark (Handling uncertainties via a tractable approach)**.** *Unlike the direct application of ADMM for the provision of real-time market services from air conditioners, our approach further extends the scope to address the effect of uncertainties in outdoor temperature in the local controller implementation. In this regard, a closed loop MPC approach coupled with a causal disturbance feedback policy is utilised. This alleviates the conservatism associated with the consideration of worst-case uncertainty in outdoor temperature. Most importantly, the overall robust control approach is tractable and can be easily solved with existing commercial solvers. In addition to that, the receding horizon control implementation can also capture uncertainties associated with each air conditioning subsystem to a certain extent.*

Besides, this conceptual framework readily allows cost-effective local controller implementation by embedding as an additional control feature in typical home energy management systems [37]. The overall control scheme is explained in Algorithm 1 in Appendix E.

4. Results

In order to validate the proposed approach, it is assumed that the DR aggregator receives a load-set point reference signal which should be tracked for $T_{\text{dur}} = 2$

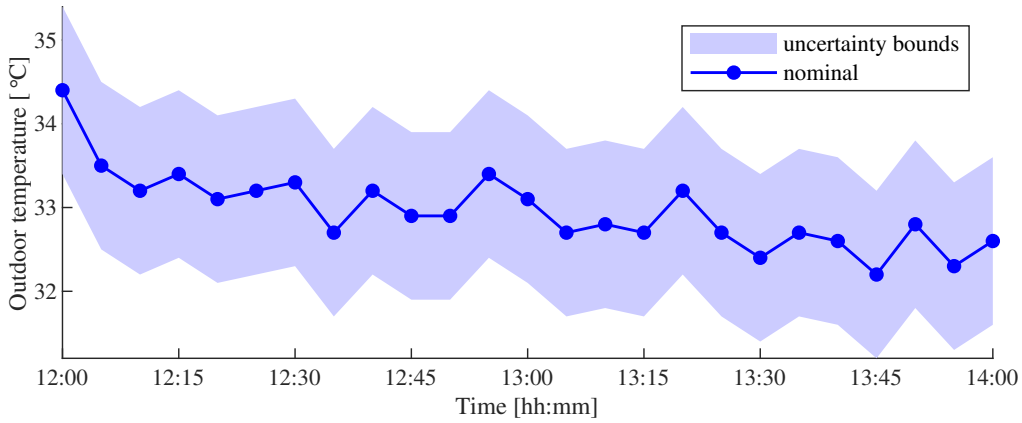

Fig. 4. The nominal variation of outdoor temperature and a range forecast with $\hat{v} = 1°C$

hr, from 12:00 - 14:00 on 02 February 2020. The nominal outdoor temperature profile obtained from [38] is given in Fig. 4. Assuming that all the households are spread across the same geographical region, the nominal outdoor temperature profile is assumed to be the same.

The load set-point signal is constructed from the scheduled generation and demand data obtained from [39]. First, the scheduled generation is compared against the demand and thereafter normalised. Next, the baseline consumption is calculated as in [7] by assuming the desired set-point temperature to be 23°C. Finally, the overall load set-point signal is constructed by combining the normalised reference signal and assuming 15% regulation capacity from the baseline consumption.

The upper limit of power consumption ($\overline{u}_i \, \forall \, i$) is considered to be normally distributed between 2.5 $\sim$ 3.5 kW and the lower limit ($\underline{u}_i \, \forall \, i$) is assumed to be zero. Aligned with [26], $R_i \; \forall \, i$ is assumed to be normally distributed between 1.5 $\sim$ 2.5°C/kW; $C_i \; \forall \, i$ is normally distributed between 1.5 $\sim$ 2.5 kWh/°C; η_i =2.5 for all the air conditioners; The lower-thermal comfort limit, $\underline{x}$ = 22°C; upper-limit $\overline{x}$ = 24°C; for all the air conditioners. The initial indoor temperature $x_i(k|k) \, \forall \, i$ is assumed to be 23°C. Assuming that end-users are *price-takers* and therefore can respond to real-time prices, the spot price of electricity obtained from [39] is employed in the household local controller problem (15).

For the MPC scheme, the sampling time (Δ) is chosen to be 5-mins to comply with the operation of the National Electricity Market (NEM) [39]; the prediction horizon (N) is chosen to be 15-mins. For the ADMM scheme, ρ = 1, $\epsilon^r = \epsilon^s =$ `1e-3`. The algorithms are written in MATLAB 2019a together with *YALMIP* toolbox [40] and *Gurobi 8.0.1* [41] is used as the solver on a computing

facility equipped with Intel(R) Xeon(R) CPU E5-2680 v3 2.50GHz and 64 GB RAM memory.

In order to assess the effect of uncertainties on the performance of the overall control scheme, simulations are carried out for the following scenarios based on the degree of uncertainty associated with outdoor temperature ($\hat{v}$) in each household local controller problem described in section 3.2:

- *Scenario 1*: the nominal scenario where perfect predictions of outdoor temperature are available at each household local controller level, i.e., the case where the outdoor temperature profile is unaffected by uncertainties.
- *Scenario 2*: the outdoor temperature profile is affected by uncertainties such that $\hat{v}_i = 0.5°\text{C}$ for all i
- *Scenario 3*: the outdoor temperature profile is affected by uncertainties such that $\hat{v}_i = 1.0°\text{C}$ for all i

for a population of $n = 500$ where each local controller attempts to minimise the cost of consumption of electricity described in (15). It is worth mentioning that, in the absence of uncertainties, i.e., the nominal scenario, the local controller robust MPC problem (15) boils down to a simple quadratic programming problem.

The load set-point tracking performance of the proposed hierarchical robust MPC scheme under different scenarios is depicted in Fig. 5. According to that, the tracking performance is found to be nearly identical for all the scenarios. Analytical calculation of mean absolute error (MAE) results in 0.0051 kW, 0.0054 kW, 0.0055 kW for *Scenario 1*, *Scenario 2* and *Scenario 3* respectively. Although MAE tends to increase as the tightness of $\hat{v}$ is reduced, much smaller values relative to the load set-point signal suggests that tracking performance of the proposed distributed control scheme is resilient against uncertainties in outdoor temperature forecasts.

Moving on to the corresponding indoor temperature and power consumption plots, it can be seen from Fig. 6 that under *Scenario 1*, *Scenario 2* and *Scenario 3*, the proposed control scheme is able to preserve thermal comfort for end-users by managing the operation within preferred thermal limits $[22 \sim 24]°\text{C}$. A closer inspection of the corresponding power consumption profiles also suggest that air conditioners tend to follow an identical profile for most part of the operation. This clearly gives the intuition behind the ADMM approach in *sharing problem*, where identical control actions are implemented across the population of air conditioners in order to reach consensus. However, the periods where air conditioners

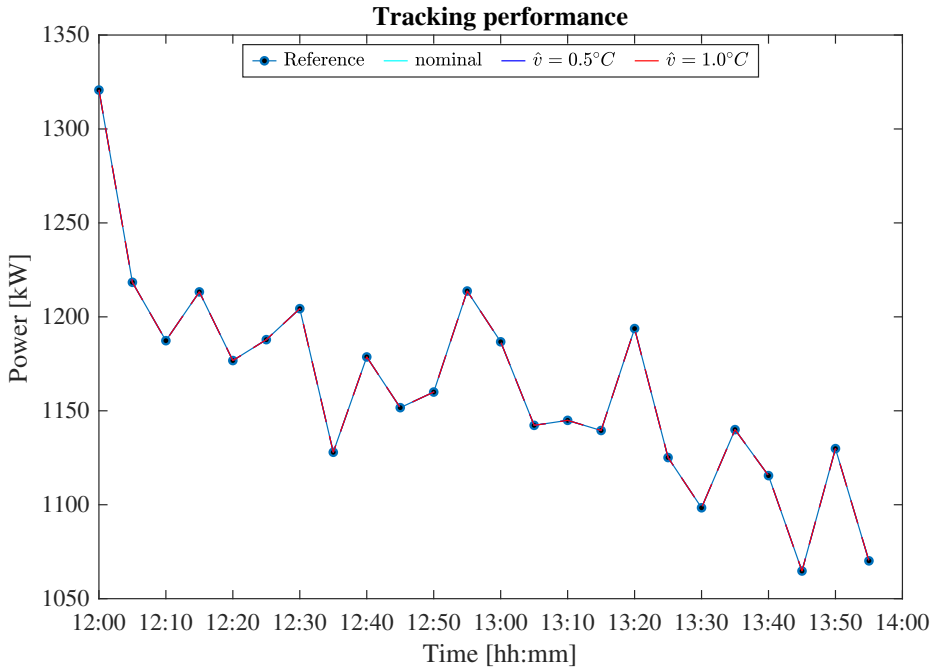

Fig. 5. The tracking performance for $n = 500$ under *Scenario 1*; *Scenario 2* and *Scenario 3*. The MAE for *Scenario 1*: 0.0051 kW; *Scenario 2*: 0.0054 kW and *Scenario 3*: 0.0055 kW.

tend to deviate from the consensus-based profile, are to manage the indoor temperature within preferred limits. For example, when the local MPC controller foresees a violation of indoor temperature limits if the control inputs follow the ADMM-based profile in a future step, it steers the control set-point away from the consensus-based profile to maintain the operation within preferred thermal limits. Even though this will lead to a mismatch in the aggregate tracking performance, the air conditioners which have the capacity to provide additional response without violating thermal limits, e.g., air conditioners with high R and C, actively adjust their consumption to achieve desired tracking performance. Likewise, the overall control scheme can provide desired tracking performance while ensuring that end-user thermal comfort is not compromised.

Comparing the simulation results to study the effect of uncertainties, it is observed that the response rate of reaching thermal bounds is slower for the nominal scenario as compared to *Scenario 2* and *Scenario 3*. Thus, fewer fluctuations of the power consumption profiles from the desired profile is observed as in Fig. 6a. Nevertheless, as the degree of uncertainty increases, the randomness of the indoor

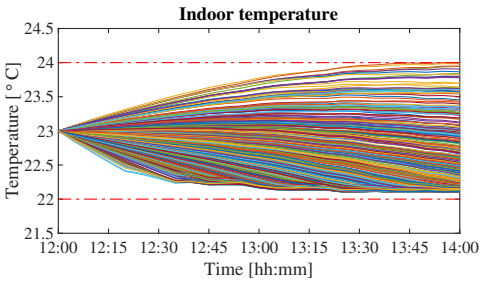

(a) *Scenario* 1:Nominal scenario

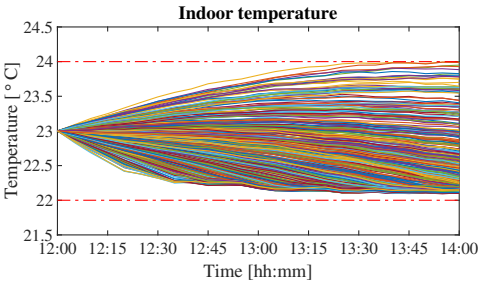

(b) *Scenario 2*: with $\hat{v}$ = 0.5°C

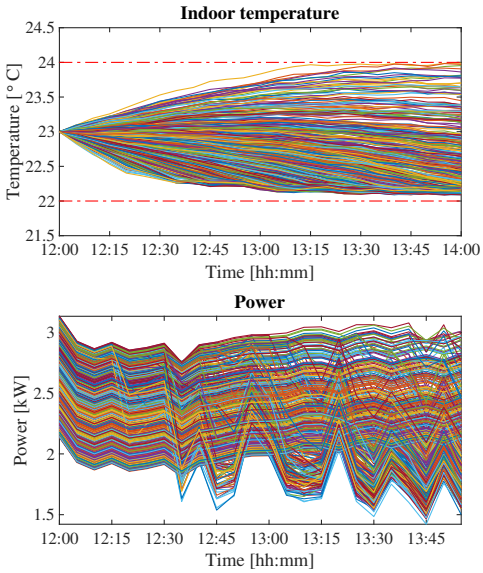

(c) *Scenario 3*: with $\hat{v}$ = 1.0°C

Fig. 6. The variation of indoor temperature and power consumption of air conditioners for *Scenario 1* (a); *Scenario 2* (b); *Scenario 3* (c) with n = 500.

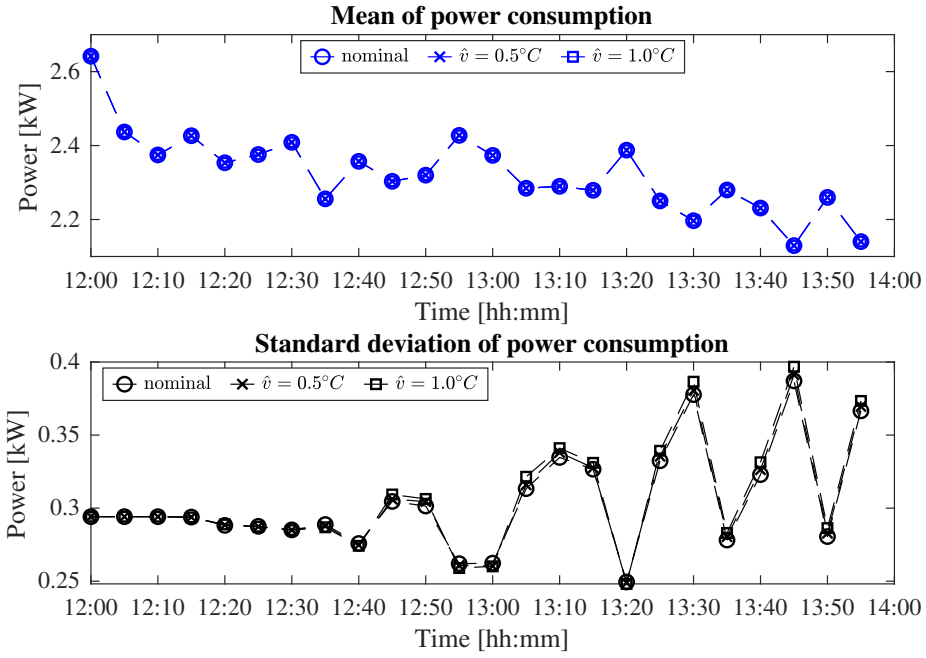

Fig. 7. The variation of mean and standard deviation of power consumption of air conditioners for *Scenario 1*; *Scenario 2*; *Scenario 3* with $n = 500$.

temperature profile for air conditioners tends to increase as seen in Fig. 6b and Fig. 6c. This will result in some air conditioners reaching their thermal limits much earlier than the nominal scenario as seen in the indoor temperature profile for *Scenario 2* and *Scenario 3*. To this end, the robust MPC controller at each house follows a non-conservative approach whereby the consumption sufficiently controlled to mitigate indoor temperature violations. This is clearly seen in the power consumption profile after 13:15 for *Scenario 2* and *Scenario 3*, where frequent fluctuations in power consumption profiles are observed compared to the nominal scenario. Nonetheless, the tracking performance is still maintained with additional power adjustments provided by many of the air conditioners operating closer to the temperature set-point. This is counteractive to the conventional approach where control set-points are determined considering the worst-case outdoor temperature variations even if the indoor temperature remains closer to the nominal set-point. To summarise, larger the bounds of uncertainty in outdoor temperature, greater it compromises the tracking performance of the overall control scheme.

Looking at Fig. 7, it is evident that the mean consumption of air-conditioners remains unchanged for all the scenarios and tend to follow a profile similar to the reference set-point signal in Fig. 5. This can be explained with the principle behind the ADMM formulation of the sharing problem where consensus is reached when local controllers set the power consumption at the mean value of the population. On the other hand, the profile of standard deviation varies for each scenario approximately after 12:40 depending on the number of devices that deliberately adjust their consumption from the identical profile to mitigate thermal comfort violations. In fact, divergence from the nominal standard deviation profile gets larger as the degree of uncertainty in outdoor temperature increases.

Additionally, one could argue that the proposed scheme will deliver desired load set-point tracking performance only in the presence of a robust outdoor temperature forecasting algorithm, i.e., under tight bounds of $\hat{v}$. However, under a short MPC prediction horizon (N = 15-mins), the outdoor temperature deviations are likely to be negligible due to slow thermal dynamics relative to power tracking dynamics. Not only that, the feedback loop inherent in the MPC scheme itself will also account for mismatches in outdoor temperature over the prediction horizon (N). Nevertheless, to give the reader a flavour of the accuracy of existing outdoor temperature forecasting algorithms, Bureau of Meteorology (BoM) – Australia can forecast outdoor temperature up to an accuracy of 2°C from the actual value [42]. With regard to the determination of uncertainty bounds, error metrics such as maximum absolute error, standard deviation can be used in the presence of an outdoor temperature forecasting algorithm. Alternatively, historical data on outdoor temperature measurements can be accommodated in estimating the bounds of uncertainty in the absence of a forecasting algorithm.

5. Discussion

The computational performance of the overall control scheme, the convergence behaviour of the ADMM-based implementation, the benefits of the proposed scheme over existing work in preserving thermal comfort and the efficacy of the proposed approach in minimising consumption and emission costs are discussed in detail in the following sections.

5.1. Scalability of the approach

Considering a scenario where the DR aggregator tracking the reference signal in real-time for T_{dur} = 2 hours, the total time taken by the proposed control

algorithm for the overall execution of the task, i.e., total execution time, under different scenarios is summarised in Table 2.

Table 2. Comparison of the total execution time for different scenarios under different aggregation sizes (n)

Aggregation size (n)	Total execution time under the nominal scenario (min)	Total execution time in the presence of uncertainties (min)	
		$\hat{v} = 0.5$°C	$\hat{v} = 1.0$°C
100	4.748	5.135	5.478
500	19.85	20.31	20.31
1000	39.51	40.38	40.23

¯ simulations are performed on a computing facility equipped with Intel(R) Xeon(R) CPU E5-2680 v3 2.50GHz and 64 GB RAM memory.
¯ based on parallel execution of the local controller problem (15).

It is evident from Table 2 that the proposed control algorithm is able to complete the overall execution of tracking the reference signal in real-time within 2 hours = 120 mins, under all the scenarios. Hence, it can be concluded that the overall control approach is scalable. What is interesting about the data in the table is that the proposed robust hierarchical control scheme is able to solve the tracking problem in approximately linear time for $\hat{v} = 0.5$°C and $\hat{v} = 1.0$°C. This gives a clear intuition that unlike the conventional robust min-max MPC approach which is computationally intractable, the causal disturbance feedback control policy employed in this work is able to determine a tractable solution to the local controller robust MPC problem at each sampling instant of the overall control operation. Moreover, the computational performance under $\hat{v} = 0.5$°C and $\hat{v} = 1.0$°C is even closer to the nominal scenario where a simple quadratic programming problem is solved at each local controller. It is also worth mentioning that unlike the execution of the overall control algorithm on a single computing facility as followed in the work, the cyber-physical implementation is arranged such that each local controller and the coordinating controller execute their own algorithms independently. In fact, this will further enhance the scalability of the overall approach for aggregations even beyond $n = 1000$.

On the other hand, Table 2 only provides information on the computational performance of the overall approach for the uncertainty in outdoor temperature

varying such that $\hat{v} = 0.5$°C and $\hat{v} = 1.0$°C. In fact, these bounds of uncertainty are aligned with the typical forecast accuracy attained by the BoM [42]. Again, this is obvious as ±1.5 °C and ±2.0 °C deviations of outdoor temperature from the nominal value is far-from reality when an MPC prediction horizon of 15-mins is considered. Nonetheless, given thermal comfort limits for end-users, the proposed approach can be employed to determine a performance bound, i.e., the degree of uncertainty in outdoor temperature up to which the overall problem results in a feasible solution.

5.2. Convergence of the ADMM algorithm

The convergence of the primal residual (**r**) and the dual residual (**s**) for $n = 500$ under the *Scenario 2* is illustrated in Fig. 8.

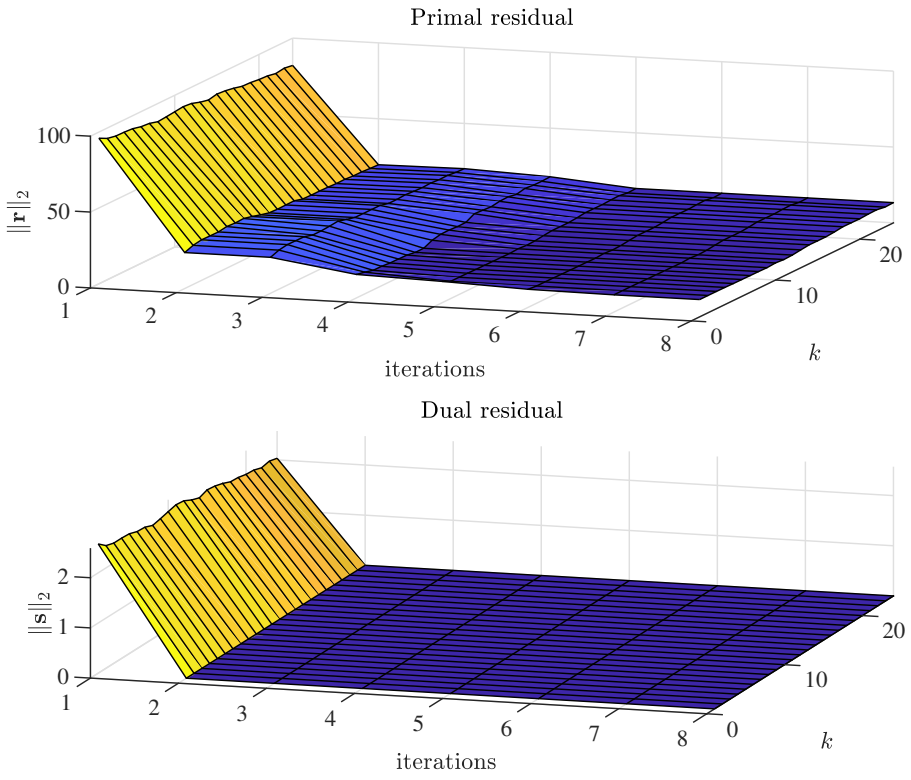

Fig. 8. Convergence of the primal residual (**r**) and the dual residual (**s**) for *Scenario 2* under $n = 500$

It is evident from Fig. 8 that the primal residual saturates around the 5^{th} iteration whereas the dual residual reaches the lower-bound $\epsilon^s = 1e-3$, after the second iteration at each sampling instant denoted by k. Since a receding horizon control framework is implemented in this work, the ADMM convergence criteria described in section 3.4 should be met at each sampling instant before the next step is reached. In this regard, the saturation of the primal residual results in the iterative algorithm failing to progress at a certain step before the overall system is updated at the next sampling instant which is 5-mins. To this end, the technique *double termination criteria* can be utilised. In other words, an additional termination criteria can be employed for the overall scheme along with (17). One such alternative criteria would be to introduce an upper-bound on maximum ADMM iterations at a certain step. However, such an upper-bound should be chosen with care as there is always a trade-off between the tracking performance and the total execution time under the decision of termination criteria in ADMM.

5.3. Comparison with existing approaches

The proposed ADMM-based robust MPC approaches is compared with two other commonly found approaches: 1) end-user thermal constraints are explicitly considered whereas the robustness to uncertainties is not explicitly considered; 2) both end-user thermal constraints and robustness to uncertainties are not explicitly considered. It is worth highlighting that the majority of existing work in Table 1, for example, [13, 14, 16, 17] fall into the category where the effect of uncertainties are neglected even though end-user thermal constraints are explicitly considered.

Table 3. Comparison of thermal comfort preservation and feasibility of the control scheme with and without robustness against uncertainties in outdoor temperature for $n = 500$ under *Scenario 2* and *Scenario 3*

Approach	Thermal comfort preserved?		Feasibility of MPC	
	$\hat{v} = 0.5°C$	$\hat{v} = 1.0°C$	$\hat{v} = 0.5°C$	$\hat{v} = 1.0°C$
w/o robust MPC (w/ thermal constraints)	✓	✓	×	×
w/o robust MPC (w/o thermal constraints)	×	×	✓	✓
proposed	✓	✓	✓	✓

It can be seen from the data in Table 3 that, although end-user thermal comfort limits are considered, the absence of knowledge on the uncertainty in outdoor temperature leads to an infeasible MPC problem in the first approach. For instance,

the MPC scheme reaches infeasibility at 13:55 under $\hat{v} = 0.5$°C and at 13:45 under $\hat{v} = 1.0$°C. This is because the uncertainty in outdoor temperature pushes indoor temperature towards lower (22°C) and upper (24°C) margins and the MPC scheme is no longer able to adjust power consumption to mitigate temperature violations beyond a certain point. On the other hand, when indoor temperature constraints are dropped, feasibility of the MPC scheme is guaranteed in the presence of uncertainties at the expense of end-user thermal comfort violations. For instance, 163 out of 500 and 165 out of 500 households experience thermal comfort violations under $\hat{v} = 0.5$°C and $\hat{v} = 1.0$°C respectively. These temperature violations will grow further as the uncertainty bound ($\hat{v}$) increases. On the contrary, the proposed approach ensures a feasible MPC problem while preserving end-user thermal comfort limits under partial knowledge of uncertainty in outdoor temperature.

To evaluate the effectiveness of the proposed approach in minimising costs, the cost of purchasing electricity in the absence of a DR event is calculated with the aid of average spot price on 02 February 2020 obtained from [39] and then compared against cost of purchasing electricity under the influence of a DR event for a period of 2 hours from 12:00 to 14:00. This results in an hourly saving of 37.60 A$ (Australian Dollars) which is equivalent to a 54.8% cost reduction compared to the base case with 500 air-conditioning units. On the other hand, the CO_2 emission factor for Queensland obtained from [43] is used to obtain a measure of emission savings by replacing the typical grid operation with end-user demand management. This equates to an average reduction of 944.14 kg CO_2-e/hr during the DR event. Therefore, it can be concluded that the proposed demand management scheme is cost-beneficial for and climate-friendly.

6. Conclusion

In this study, an end-user privacy and thermal comfort preserving, hierarchical control scheme based on ADMM and robust MPC is proposed for the control of inverter-type air conditioners to provide real-time electricity market services in the presence of uncertainties. Under the proposed hierarchical control framework, a local controller at each household minimises the cost of consumption of electricity associated with the air conditioner in the presence of outdoor temperature forecast errors whereas a coordinating controller at the DR aggregator ensures that the collective response from air conditioners follow the market operator specified load set-point signal. The overall control scheme is validated using real data obtained

from the Australian Energy Market Operator (AEMO). Some of the key insights gained from the study are as follows:

- The overall control scheme is able to achieve precise tracking of the load-set point signal with mean absolute error less than 0.0055 kW up to $\pm 1^{\circ}$C variation of outdoor temperature from its forecasted value.
- The closed-loop MPC approach based on a causal disturbance feedback policy is non-conservative as well as tractable. Furthermore, the approach can achieve the same level of computational performance of the scenario where perfect predictions of outdoor temperature are available. This is a notable improvement over the conventional worst-case min-max MPC approach.
- Given end-user thermal comfort limits, the proposed control scheme can be employed to determine a performance bound on handling uncertainties associated with outdoor temperature.
- A cost-beneficial real-world implementation of the household local controller can be realised by embedding its control features in existing home energy management systems.

The findings of this study will be of importance to retailers and DR aggregators in devising advanced control architectures to maximise their social welfare in future electricity markets where active participation of consumer-owned DERs is prevalent.

The future work will be to extend the control capabilities of the proposed approach to account for factors such as: external disturbances due to humidity, mismatches in the estimation of household thermal parameters. In addition to that, enhancing the resilience of the overall control approach against latency and imperfections in the bidirectional communication infrastructure is also an interesting research direction.

Appendix A. Representation of vectors in the state prediction dynamics and output prediction dynamics of the aggregate system

For the aggregate system, the input vector $\mathbf{u}(k)$, exogenous input vector $\tilde{\mathbf{v}}(k)$, stochastic additive disturbance vector $\mathbf{w}(k)$ in the state prediction dynamics and

$\mathbf{y}(k)$ in the output prediction dynamics can be expressed as given below.

$$\begin{aligned}
\mathbf{u}(k) &= \left[\mathbf{u}^{\mathrm{T}}(k|k), \ldots, \mathbf{u}^{\mathrm{T}}(k+N-1|k)\right]^{\mathrm{T}} \in \mathbb{R}^{nN} \\
\tilde{\mathbf{v}}(k) &= \left[\tilde{\mathbf{v}}^{\mathrm{T}}(k|k), \ldots, \tilde{\mathbf{v}}^{\mathrm{T}}(k+N-1|k)\right]^{\mathrm{T}} \in \mathbb{R}^{nN} \\
\mathbf{w}(k) &= \left[\mathbf{w}^{\mathrm{T}}(k|k), \ldots, \mathbf{w}^{\mathrm{T}}(k+N-1|k)\right]^{\mathrm{T}} \in \mathbb{R}^{nN} \\
\mathbf{y}(k) &= \left[\mathbf{y}^{\mathrm{T}}(k|k), \ldots, \mathbf{y}^{\mathrm{T}}(k+N|k)\right]^{\mathrm{T}} \in \mathbb{R}^{n(N+1)}
\end{aligned}$$

Appendix B. Compact state prediction model of the aggregate system

For the compact state prediction of the overall model described by (3), the matrices $\mathbf{A} \in \mathbb{R}^{n(N+1)\times n}, \mathbf{B}, \mathbf{D}, \mathbf{G} \in \mathbb{R}^{n(N+1)\times nN}$ and $\mathbf{E} \in \mathbb{R}^{n(N+1)\times n(N+1)}$ such that,

$$\mathbf{A} = \begin{bmatrix} \mathbb{I}_n \\ A \\ A^2 \\ \vdots \\ A^N \end{bmatrix} \quad \mathbf{B} = \begin{bmatrix} B & \mathbf{0} & \cdots & \cdots & \cdots \\ AB & B & \mathbf{0} & \cdots & \cdots \\ A^2B & AB & B & \mathbf{0} & \cdots \\ \vdots & \vdots & \vdots & \ddots & \vdots \\ A^NB & A^{N-1}B & \cdots & \cdots & \ddots \end{bmatrix}$$

$$\mathbf{D} = \begin{bmatrix} D & \mathbf{0} & \cdots & \cdots & \cdots \\ AD & D & \mathbf{0} & \cdots & \cdots \\ A^2D & AD & D & \mathbf{0} & \cdots \\ \vdots & \vdots & \vdots & \ddots & \vdots \\ A^ND & A^{N-1}D & \cdots & \cdots & \ddots \end{bmatrix} \quad \mathbf{G} = \begin{bmatrix} \mathbb{I}_n & \mathbf{0} & \cdots & \cdots & \cdots \\ A & \mathbb{I}_n & \mathbf{0} & \cdots & \cdots \\ A^2 & A & \mathbb{I}_n & \mathbf{0} & \cdots \\ \vdots & \vdots & \vdots & \ddots & \vdots \\ A^N & A^{N-1} & \cdots & \cdots & \ddots \end{bmatrix}$$

and $\mathbf{E} = E \otimes \mathbb{I}_{N+1}$.

Appendix C. Tractable formulation of the closed-loop MPC with a causal disturbance feedback policy

Considering the ith air conditioning subsystem, the state and input constraints can be represented in a compact form as:

$$\begin{aligned}
\mathcal{Z}_i := \{&(x_i(k+j|k), u_i(k+j|k), v_i(k+j|k)) \in \mathbb{R}\times\mathbb{R}\times\mathbb{R} \\
&| \, \mathbb{d}_i\, x_i(k+j|k) + \mathbb{e}_i\, u_i(k+j|k) + \mathbb{f}_i\, \tilde{v}_i(k+j|k) \leq \mathbb{g}_i\}, \forall\, j \in \mathbb{Z}_{[0,N-1]}
\end{aligned} \tag{C.1}$$

where the vectors $\mathbb{d}_i, \mathbb{e}_i, \mathbb{f}_i$ and $\mathbb{g}_i \in \mathbb{R}^s$.

Furthermore, the causal disturbance feedback control policy can be expressed as:

$$u_i(k+j|k) = \sum_{m=0}^{j-1} \mathrm{T}_i(k+j|k, k+m|k) \cdot w_i(k+m|k) + \tilde{u}_i(k+j|k) \quad \forall\, j \in \mathbb{Z}_{[0,N-1]} \tag{C.2}$$

Let us define the vector $\tilde{\mathbf{u}}_i(k)$ as,

$$\tilde{\mathbf{u}}_i(k) := \left[\tilde{u}_i(k|k) \ldots, \tilde{u}_i(k+N-1|k)\right]^{\mathrm{T}} \in \mathbb{R}^N \tag{C.3}$$

The strictly lower triangular matrix $\mathbf{T}_i \in \mathbb{R}^{N\times N}$ as,

$$\mathbf{T}_i(k) := \begin{bmatrix} 0 & \cdots & \cdots & 0 \\ \mathrm{T}_i(k+1|k) & 0 & \cdots & 0 \\ \vdots & \ddots & \ddots & \vdots \\ \mathrm{T}_i(k+N-1|k) & \cdots & \mathrm{T}_i(k+N-1|k+N-2) & 0 \end{bmatrix} \tag{C.4}$$

Hence, the input policy (C.2) can be written in a compact form as

$$\mathbf{u}_i(k) = \mathbf{T}_i(k) \cdot \mathbf{w}_i(k) + \tilde{\mathbf{u}}_i(k) \tag{C.5}$$

Consequently, the admissible $\left(\mathbf{T}_i(k), \tilde{\mathbf{u}}_i(k)\right)$ can be defined as:

$$\Pi_i(x_i) := \left\{ \left(\mathbf{T}_i(k), \tilde{\mathbf{u}}_i(k)\right) \;\middle|\; \begin{array}{l} \left(\mathbf{T}_i(k), \tilde{\mathbf{u}}_i(k)\right) \text{satisfies (C.5)},\ x_i = x_i(k\,|\,k) \\ x_i(k+j+1|k) = A_i x_i(k+j|k) + B_i u_i(k+j|k) \\ \qquad\qquad + D_i \tilde{v}_i(k+j\,|\,k) + w_i(k+j\,|\,k) \\ u_i(k+j|k) = \displaystyle\sum_{m=0}^{j-1} \mathrm{T}_i(k+j|k, k+m|k) w_i(k+m|k) + \\ \qquad\qquad \tilde{u}_i(k+j|k) \\ \left(x_i(k+j|k), u_i(k+j|k), \tilde{v}_i(k+j|k)\right) \in \mathcal{Z}_i \\ w_i(k+j|k) \in \mathbb{W}_i, \quad \forall\, j \in \mathbb{Z}_{[0,N-1]} \end{array} \right\} \tag{C.6}$$

Considering the state prediction dynamics for the *i*the subsytem,:

$$\mathbf{x}_i(k) = \mathbf{A}_i\, \mathbf{x}_i(k|k) + \mathbf{B}_i\, \mathbf{u}_i(k) + \mathbf{D}_i\, \tilde{\mathbf{v}}_i(k) + \mathbf{G}_i\, \mathbf{w}_i(k) \tag{C.7}$$

$$\mathbf{y}_i(k) = \mathbf{E}_i\, \mathbf{x}_i(k) \tag{C.8}$$

where $\mathbf{A}_i \in \mathbb{R}^N$ can be derived from the overall state prediction dynamics given in Appendix B as $\mathbf{A}_i = \left[1, A_i, A_i^2, \ldots, A_i^{N-1}\right]^{\mathrm{T}}$. Similarly, $\mathbf{B}_i, \mathbf{D}_i, \mathbf{G}_i \in \mathbb{R}^{N\times N}$ and $\mathbf{E}_i = \mathbb{I}_N$ can be obtained.

Now define $\mathbb{D}_i := \mathbb{d}_i \otimes \mathbb{I}_N$, $\mathbb{E}_i := \mathbb{e}_i \otimes \mathbb{I}_N$, $\mathbb{F}_i := \mathbb{f}_i \otimes \mathbb{I}_N$ and $\mathbb{G}_i := \mathbb{g}_i \otimes \mathbb{I}_N$. Then the predicted state and input constraints can be written as:

$$\mathbb{D}_i\, \mathbf{x}_i(k) + \mathbb{E}_i\, \mathbf{u}_i(k) + \mathbb{F}_i\, \tilde{\mathbf{v}}_i(k) \leq \mathbb{G}_i \tag{C.9}$$

Substituting the predicted state dynamics $\mathbf{x}_i(k) = \mathbf{A}_i x_i(k|k) + \mathbf{B}_i \mathbf{u}_i(k) + \mathbf{D}_i \tilde{\mathbf{v}}_i(k) + \mathbf{G}_i \mathbf{w}_i(k)$ in (C.9) yields:

$$(\mathbb{D}_i\, \mathbf{B}_i + \mathbb{E}_i) \cdot \mathbf{u}_i(k) + \mathbb{D}_i\, \mathbf{G}_i \cdot \mathbf{w}_i(k) + (\mathbb{D}_i\, \mathbf{D}_i + \mathbb{F}_i) \cdot \tilde{\mathbf{v}}_i(k) \leq \mathbb{G}_i - \mathbb{D}_i\, \mathbf{A}_i\, x_i(k|k)$$

Substituting $\mathbb{J}_i = \mathbb{D}_i\, \mathbf{B}_i + \mathbb{E}_i$, $\mathbb{K}_i = \mathbb{D}_i\, \mathbf{G}_i$, $\mathbb{L}_i = \mathbb{D}_i\, \mathbf{D}_i + \mathbb{F}_i$, $\mathbb{M}_i = -\mathbb{D}_i\, \mathbf{A}_i$ and also substituting (C.5) gives,

$$\mathbb{J}_i\, \tilde{\mathbf{u}}_i(k) + (\mathbb{J}_i\, \mathbf{T}_i(k) + \mathbb{K}_i) \cdot \mathbf{w}_i(k) \leq \mathbb{G}_i + \mathbb{M}_i\, \mathbf{x}_i(k|k) - \mathbb{L}_i\, \tilde{\mathbf{v}}_i(k) \tag{C.10}$$

Hence, the admissible set can be written as:

$$\mathit{\Pi}_i(x_i) := \left\{ \left(\mathbf{T}_i(k), \tilde{\mathbf{u}}_i(k)\right) \;\middle|\; \begin{array}{l} \left(\mathbf{T}_i(k), \tilde{\mathbf{u}}_i(k)\right) \text{satisfies (C.5)} \\ \mathbb{J}_i\, \tilde{\mathbf{u}}_i(k) + \\ \underset{\mathbf{w}_i(k)\in\, \mathbb{W}_i^N}{max}\, (\mathbb{J}_i \mathbf{T}_i(k) + \mathbb{K}_i)\, \mathbf{w}_i(k) \leq \mathbb{G}_i + \mathbb{M}_i \mathbf{x}_i(k|k) - \mathbb{L}_i \tilde{\mathbf{v}}_i(k) \end{array} \right\} \tag{C.11}$$

Note that the uncertainty associated with outdoor temperature is bounded such that,

$$\mathbb{W}_i = \{w_i \text{ s.t. } |w_i| \leq D_i \cdot \hat{v}_i\} \tag{C.12}$$

In addition to that, $w_i(k) = D_i \cdot \grave{v}_i(k)$ at time step k, where $\grave{v}_i(k) \in [-\hat{v}_i, \hat{v}_i]$ is the deviation of actual outdoor temperature from the nominal value at kth sampling instant.

Define $\grave{\mathbf{v}}_i(k) = \left[\grave{v}_i(k|k), \ldots, \grave{v}_i(k+N-1|k)\right]^{\mathrm{T}} \in \mathbb{R}^N$ and define $J_i := \mathbf{G}_i \in \mathbb{R}^{N\times N}$ such that $\mathbf{w}_i(k) = J_i\, \grave{\mathbf{v}}_i(k)$. By applying dual norm and row-wise maximisation, (C.11) simplifies to:

$$\mathit{\Pi}_i(x_i) := \left\{ \left(\mathbf{T}_i(k), \tilde{\mathbf{u}}_i(k)\right) \;\middle|\; \begin{array}{l} \left(\mathbf{T}_i(k), \tilde{\mathbf{u}}_i(k)\right) \text{satisfies (C.5)} \\ \mathbb{J}_i\, \tilde{\mathbf{u}}_i(k) + |\mathbb{J}_i \mathbf{T}_i(k)\, J_i + \mathbb{K}_i\, J_i| \mathbf{1} \leq \mathbb{G}_i + \mathbb{M}_i \mathbf{x}_i(k|k) - \mathbb{L}_i \tilde{\mathbf{v}}_i(k) \end{array} \right\} \tag{C.13}$$

Note that, $x_i(k|k)$ is the initial indoor temperature and $\tilde{\mathbf{v}}_i(k)$ is the nominal variation of outdoor temperature which are available as priori information.

Thereafter, adding slack variables to replace the absolute operator in (C.13) gives:

$$\Pi_i(x_i) := \left\{ \Big(\mathbf{T}_i(k), \tilde{\mathbf{u}}_i(k)\Big) \;\middle|\; \begin{array}{l} \Big(\mathbf{T}_i(k), \tilde{\mathbf{u}}_i(k)\Big) \quad \text{satisfies (C.5)}, \;\; \exists\, \mathbf{\Psi}_i \text{ s.t.} \\ \mathbb{J}_i\, \tilde{\mathbf{u}}_i(k) + \mathbf{\Psi}_i\, \mathbf{1} \leq \mathbb{G}_i + \mathbb{M}_i x_i(k|k) - \mathbb{L}_i \tilde{\mathbf{v}}_i(k) \\ -\mathbf{\Psi}_i \leq (\mathbb{J}_i\, \mathbf{T}_i(k)\, J_i + \mathbb{K}_i\, J_i) \leq \mathbf{\Psi}_i \end{array} \right\} \tag{C.14}$$

The admissible set in (C.14) is composed of affine constraints of $(\mathbf{T}_i(k), \tilde{\mathbf{u}}_i(k),\ \mathbf{\Psi}_i)$, hence convex.

Consequently, the closed loop robust MPC problem can be reformulated as a convex programming problem as follows:

$$\min_{\mathbf{T}_i, \tilde{\mathbf{u}}_i, \mathbf{\Psi}_i} \quad \sum_{j=0}^{N-1} \Big[\, \ell_{i,j}\Big(x_i(k+j\,|\,k), \tilde{u}_i(k+j\,|\,k)\Big) + (\rho/2)\Big(\tilde{u}_i(k+j|k) - \tilde{u}_i^{(\nu)}(k+j) + \overline{\tilde{u}}^{(\nu)}(k+j) - \overline{z}^{(\nu)}(k+j) + \theta^{(\nu)}(k+j)\Big)^2 \Big] \tag{C.15a}$$

subject to:

$$\mathrm{T}_i(k+j\,|\,k, k+m\,|\,k) = 0 \qquad \forall\, j \leq m \tag{C.15b}$$

$$\mathbb{J}_i\, \tilde{\mathbf{u}}_i(k) + \mathbf{\Psi}_i\, \mathbf{1} \leq \mathbb{G}_i + \mathbb{M}_i\, \mathbf{x}(k|k) - \mathbb{L}_i\, \tilde{\mathbf{v}}_i(k) \tag{C.15c}$$

$$-\mathbf{\Psi}_i \leq (\mathbb{J}_i\, \mathbf{T}_i(k)\, J_i + \mathbb{K}_i\, J_i) \leq \mathbf{\Psi}_i \tag{C.15d}$$

where $\mathbf{T}_i \in \mathbb{R}^{N\times N}$,$\tilde{\mathbf{u}}_i \in \mathbb{R}^N$ and $\mathbf{\Psi}_i \in \mathbb{R}^N$ are the decision variables. ■

Appendix D. Convergence of the overall algorithm

Based on the receding horizon implementation for the *sharing problem* in ADMM form, the primal residual (**r**) and the dual residual (**s**) for νth iteration at kth sampling instant can be expressed as:

$$\mathbf{r}^{(\nu)}(k) = \Big[\tilde{u}_1^{(\nu)}(k|k) - \overline{z}^{(\nu)}(k|k), \ldots, \tilde{u}_1^{(\nu)}(k+N-1|k) - \overline{z}^{(\nu)}(k+N-1|k), \ldots, \tilde{u}_n^{(\nu)}(k|k) - \overline{z}^{(\nu)}(k|k), \ldots, \tilde{u}_n^{(\nu)}(k+N-1|k) - \overline{z}^{(\nu)}(k+N-1|k)\Big] \tag{D.1}$$

$$\mathbf{s}^{(\nu)}(k) = -\rho\Big(\overline{z}^{(\nu+1)}(k|k) - \overline{z}^{(\nu)}(k|k), \ldots, \overline{z}^{(\nu+1)}(k+N-1|k) - \overline{z}^{(\nu)}(k+N-1|k)\Big) \tag{D.2}$$

Algorithm 1: The proposed approach based on ADMM and robust MPC

Input: T_{dur}, $P_{\text{ref}}(k+j)$, $\tilde{v}(k+j)$ for $j \in \mathbb{Z}_{[0,T_{\text{dur}}-1]}$, step-size Δ, prediction horizon N

Initialise ρ, ϵ^r, ϵ^s for ADMM;
for $\tau = k : k + T_{\text{dur}} - 1$ **do**
  set $\nu = 1$;
  Initialise $\tilde{u}_i^{(\nu)}, z_i^{(\nu)}\ \forall\ i, \theta^{(\nu)}$;
  Calculate $\overline{\tilde{u}}^{(\nu)}$ and $\overline{z}^{(\nu)}$;
  do
    for $i = 1 : n$ **do**
      function *Local controller problem:*
        Input: A_i, B_i, D_i, E_i $\underline{u}_i$, $\overline{u}_i$, $\underline{y}_i$, $\overline{y}_i$
        Solve subproblem LC_i given by (C.15);
        Send $\tilde{u}_i^{(\nu)}(\tau + j)$ for $j \in \mathbb{Z}_{[0,N-1]}$ to the coordinating controller as in step ①;
      end
    end
    function *Coordinating controller problem:*
      Determine $\overline{z}^{(\nu+1)}(\tau + j)$ for $j \in \mathbb{Z}_{[0,N-1]}$ by solving (16a);
      Update $\theta^{(\nu+1)}(\tau + j)$ for $j \in \mathbb{Z}_{[0,N-1]}$ as in (16b);
      Broadcast $[\overline{z}^{(\nu+1)}(\tau + j), \theta^{(\nu+1)}(\tau + j)]$ for $j \in \mathbb{Z}_{[0,N-1]}$ among local controllers as in step ②;
    end
    set $\nu = \nu + 1$;
  while $(\mathbf{r}^{(\nu-1)}(\tau) \leq \epsilon^r) \wedge (\mathbf{s}^{(\nu-1)}(\tau) \leq \epsilon^s)$;
  for $i = 1 : n$ **do**
    function *MPC update:*
      Apply the first control input $u_i^{(\nu^*)}(\tau)$ as in step ③;
      Measure $y_i(\tau)$ and update LC_i as in step ④;
    end
  end
end

Appendix E. The overall algorithm for the proposed approach based on ADMM and robust MPC

Acknowledgment

The authors would like to thank for the support given by UQ Centre for Energy Innovation under the Advance Queensland grant (grant no: AQPTP01216-17RD1).

References

[1] International Renewable Energy Agency (IRENA), Trends in Renewable Energy, https://www.irena.org/Statistics/View-Data-by-Topic/Capacity-and-Generation/Statistics-Time-Series, Accessed: 20-12-2020.

[2] D. S. Callaway, Tapping the energy storage potential in electric loads to deliver load following and regulation, with application to wind energy, Energy Conversion and Management 50 (5) (2009) 1389–1400. doi:https://doi.org/10.1016/j.enconman.2008.12.012.

[3] X. Wei, A. Kusiak, M. Li, F. Tang, Y. Zeng, Multi-objective optimization of the HVAC (heating, ventilation, and air conditioning) system performance, Energy 83 (2015) 294–306. doi:https://doi.org/10.1016/j.energy.2015.02.024.
URL https://www.sciencedirect.com/science/article/pii/S0360544215001796

[4] H. Wang, S. Wang, K. Shan, Experimental study on the dynamics, quality and impacts of using variable-speed pumps in buildings for frequency regulation of smart power grids, Energy 199 (2020) 117406. doi:https://doi.org/10.1016/j.energy.2020.117406.
URL https://www.sciencedirect.com/science/article/pii/S0360544220305132

[5] N. Lu, An Evaluation of the HVAC Load Potential for Providing Load Balancing Service, IEEE Transactions on Smart Grid 3 (3) (2012) 1263–1270. doi:10.1109/TSG.2012.2183649.

[6] H. Hao, B. M. Sanandaji, K. Poolla, T. L. Vincent, Aggregate flexibility of thermostatically controlled loads, IEEE Transactions on Power Systems 30 (1) (2015) 189–198. doi:10.1109/TPWRS.2014.2328865.

[7] M. Liu, Y. Shi, Model predictive control for thermostatically controlled appliances providing balancing service, IEEE Transactions on Control Systems Technology 24 (6) (2016) 2082–2093. doi:10.1109/TCST.2016.2535400.

[8] O. Erdinç, A. Taşcikaraoğlu, N. G. Paterakis, J. P. S. Catalão, Novel Incentive Mechanism for End-Users Enrolled in DLC-Based Demand Response Programs Within Stochastic Planning Context, IEEE Transactions on Industrial Electronics 66 (2) (2019) 1476–1487. doi:10.1109/TIE.2018.2811403.

[9] F. Oldewurtel, A. Parisio, C. N. Jones, D. Gyalistras, M. Gwerder, V. Stauch, B. Lehmann, M. Morari, Use of model predictive control and weather forecasts for energy efficient building climate control, Energy and Buildings 45 (2012) 15–27. doi:10.1016/j.enbuild.2011.09.022.

[10] H. Wang, S. Wang, A hierarchical optimal control strategy for continuous demand response of building HVAC systems to provide frequency regulation service to smart power grids, Energy 230 (2021) 120741. doi:https://doi.org/10.1016/j.energy.2021.120741.

[11] T. Dengiz, P. Jochem, Decentralized optimization approaches for using the load flexibility of electric heating devices, Energy 193 (2020) 116651. doi:https://doi.org/10.1016/j.energy.2019.116651.
URL https://www.sciencedirect.com/science/article/pii/S0360544219323461

[12] Z. Dong, X. Zhang, G. Strbac, Evaluation of benefits through coordinated control of numerous thermal energy storage in highly electrified heat systems, Energy 237 (2021) 121600. doi:https://doi.org/10.1016/j.energy.2021.121600.
URL https://www.sciencedirect.com/science/article/pii/S036054422101848X

[13] A. Radaideh, A. Al-Quraan, H. Al-Masri, Z. Albataineh, Rolling horizon control architecture for distributed agents of thermostatically controlled loads enabling long-term grid-level ancillary services, International Journal of Electrical Power & Energy Systems 127 (2021) 106630. doi:https://doi.org/10.1016/j.ijepes.2020.106630.

[14] G. K. H. Larsen, N. D. van Foreest, J. M. A. Scherpen, Distributed Control of the Power Supply-Demand Balance, IEEE Transactions on Smart Grid 4 (2) (2013) 828–836. doi:10.1109/TSG.2013.2242907.

[15] S. H. Tindemans, V. Trovato, G. Strbac, Decentralized Control of Thermostatic Loads for Flexible Demand Response, IEEE Transactions on Control Systems Technology 23 (5) (2015) 1685–1700. doi:10.1109/TCST.2014.2381163.

[16] E. M. Burger, S. J. Moura, Generation following with thermostatically controlled loads via alternating direction method of multipliers sharing algorithm, Electric Power Systems Research 146 (2017) 141–160. doi:https://doi.org/10.1016/j.epsr.2016.12.001.

[17] R. Halvgaard, L. Vandenberghe, N. K. Poulsen, H. Madsen, J. B. Jørgensen, Distributed Model Predictive Control for Smart Energy Systems, IEEE Transactions on Smart Grid 7 (3) (2016) 1675–1682. doi:10.1109/TSG.2016.2526077.

[18] M. Diekerhof, F. Peterssen, A. Monti, Hierarchical Distributed Robust Optimization for Demand Response Services, IEEE Transactions on Smart Grid 9 (6) (2018) 6018–6029. doi:10.1109/TSG.2017.2701821.

[19] A. Ben-Tal, L. El Ghaoui, A. S. Nemirovski, Robust Optimization, Princeton Series in Applied Mathematics, Princeton University Press, 2009.

[20] P. Braun, T. Faulwasser, L. Grüne, C. M. Kellett, S. R. Weller, K. Worthmann, Hierarchical distributed ADMM for predictive control with applications in power networks, IFAC Journal of Systems and Control 3 (2018) 10–22. doi:https://doi.org/10.1016/j.ifacsc.2018.01.001.

[21] A. Conejo, E. Castillo, R. Minguez, R. Garcia-Bertrand, Decomposition in Nonlinear Programming, Springer Berlin Heidelberg, Berlin, Heidelberg, 2006, pp. 187–242. doi:10.1007/3-540-27686-6_5.

[22] D. Bertsimas, M. Sim, The Price of Robustness, Operations Research 52 (1) (2004) 35–53. doi:10.1287/opre.1030.0065.

[23] A. L. Soyster, Technical Note—Convex Programming with Set-Inclusive Constraints and Applications to Inexact Linear Programming, Operations Research 21 (5) (1973) 1154–1157. doi:10.1287/opre.21.5.1154.

[24] A. Gomes, C. H. Antunes, J. Martinho, A physically-based model for simulating inverter type air conditioners/heat pumps, Energy 50 (2013) 110–119. doi:https://doi.org/10.1016/j.energy.2012.11.047.

[25] M. Song, C. Gao, H. Yan, J. Yang, Thermal Battery Modeling of Inverter Air Conditioning for Demand Response, IEEE Transactions on Smart Grid 9 (6) (2018) 5522–5534. doi:10.1109/TSG.2017.2689820.

[26] J. L. Mathieu, S. Koch, D. S. Callaway, State Estimation and Control of Electric Loads to Manage Real-Time Energy Imbalance, IEEE Transactions on Power Systems 28 (1) (2013) 430–440. doi:10.1109/TPWRS.2012.2204074.

[27] D. S. Callaway, Tapping the energy storage potential in electric loads to deliver load following and regulation, with application to wind energy, Energy Conversion and Management 50 (5) (2009) 1389–1400. doi:https://doi.org/10.1016/j.enconman.2008.12.012.
URL http://www.sciencedirect.com/science/article/pii/S0196890408004780

[28] P. Du, N. Lu, Appliance commitment for household load scheduling, IEEE transactions on Smart Grid 2 (2) (2011) 411–419.

[29] X. Lu, K. Li, H. Xu, F. Wang, Z. Zhou, Y. Zhang, Fundamentals and business model for resource aggregator of demand response in electricity markets, Energy 204 (2020) 117885. doi:https://doi.org/10.1016/j.energy.2020.117885.

[30] P. O. M. Scokaert, D. Q. Mayne, Min-max feedback model predictive control for constrained linear systems, IEEE Transactions on Automatic Control 43 (8) (1998) 1136–1142. doi:10.1109/9.704989.

[31] S. Boyd, N. Parikh, E. Chu, B. Peleato, J. Eckstein, Distributed Optimization and Statistical Learning via the Alternating Direction Method of Multipliers, Found. Trends Mach. Learn. 3 (1) (2011) 1–122. doi:10.1561/2200000016.

[32] P. J. Goulart, E. C. Kerrigan, J. M. Maciejowski, Optimization over state feedback policies for robust control with constraints, Automatica 42 (4) (2006) 523–533. doi:https://doi.org/10.1016/j.automatica.2005.08.023.

[33] A. Ben-Tal, A. Goryashko, E. Guslitzer, A. Nemirovski, Adjustable robust solutions of uncertain linear programs, Mathematical programming 99 (2) (2004) 351–376.

[34] V. C. Gungor, D. Sahin, T. Kocak, S. Ergut, C. Buccella, C. Cecati, G. P. Hancke, Smart Grid Technologies: Communication Technologies and Standards, IEEE Transactions on Industrial Informatics 7 (4) (2011) 529–539. doi:10.1109/TII.2011.2166794.

[35] N. Mahdavi, J. H. Braslavsky, M. M. Seron, S. R. West, Model Predictive Control of Distributed Air-Conditioning Loads to Compensate Fluctuations in Solar Power, IEEE Transactions on Smart Grid 8 (6) (2017) 3055–3065. doi:10.1109/TSG.2017.2717447.

[36] F. Rey, X. Zhang, S. Merkli, V. Agliati, M. Kamgarpour, J. Lygeros, Strengthening the Group: Aggregated Frequency Reserve Bidding With ADMM, IEEE Transactions on Smart Grid 10 (4) (2019) 3860–3869. doi:10.1109/TSG.2018.2841508.

[37] Energex, Home Energy Management Systems, https://www.energex.com.au/home/control-your-energy/smarter-energy/home-energy-management-systems.

[38] School of Earth and Environmental Sciences, UQ weatherstations, https://bit.ly/2PXuc2n, Accessed: 20-08-2020.

[39] Australian Energy Market Operator (AEMO), National Electricity Market (NEM) DATA DASHBOARD, https://aemo.com.au/en/energy-systems/electricity/national-electricity-market-nem/data-nem/data-dashboard-nem.

[40] J. Löfberg, YALMIP : a Toolbox for Modeling and Optimization in MATLAB, in: 2004 IEEE International Conference on Robotics and Automation (IEEE Cat. No.04CH37508), 2004, pp. 284–289. doi:10.1109/CACSD.2004.1393890.

[41] Gurobi Optimization, L L C, Gurobi Optimizer Reference Manual, http://www.gurobi.com (2020).

[42] Bureau of Meteorology (BoM), Australia, Bureau Forecast Accuracy, http://www.bom.gov.au/inside/forecast-accuracy.shtml.

[43] Department of the Environment and Energy, National Greenhouse Accounts Factors, https://www.awe.gov.au/sites/default/files/documents/national-greenhouse-accounts-factors-july-2017.pdf.